

<sup>1</sup>Cristian CIOBANU, <sup>2</sup>Gheorghe VOICU, <sup>2</sup>Irina–Aura ISTRATE, <sup>2</sup>Paula VOICU, <sup>2</sup>Mariana–Gabriela MUNTEANU

## VARIATION OF ENERGY CONSUMPTION AND SPECIFIC SURFACE BLAINE RESULTING FROM SIMULATION OF CLINKER GRINDING IN A CEMENT MILL

<sup>1</sup>CEPROCIM SA, ROMANIA

<sup>2</sup>University Polytechnic of Bucharest, ROMANIA

**Abstract:** Given the technological importance of the grinding processes and the energy implications they bring, the present work sought to deepen the physics of these processes, namely: the determination of the energy consumption of the laboratory mill, the determination of the Blaine Specific Surface Area (SSA) and the variation between them. This work aimed to optimize large clinker grinding plants in the cement industry, by measuring in a laboratory mill with a rotating horizontal drum, the energy consumption, and the Blaine specific surface area. For example, clinker grinding in a laboratory ball mill was simulated by a professional simulation program EDEM 2022.0. To carry out the experiments, clinker material from a cement factory in Romania marked Clincher A was used. To carry out the experimental research, the CEPROCIM process was applied, which is based on the grinding of a batch of material in a laboratory mill with a rotating horizontal drum.

**Keywords:** grinding, specific surface, porosity, the average diameter

### INTRODUCTION

The grinding processes in the technological flow represent the main consumer of electricity in the cement industry, having a share of over 95% of the energy consumption for the whole of the grinding operations and over 70% of the total electricity consumption of this industry, (Opris, S., 1994).

The specific energy consumption of the grinding operations is accentuated by the increased resistance of the granules to the crushing efforts. Grain breakage begins in areas where cracks or other microstructural defects are found, where the material yields more easily.

As the particle sizes decrease, the probability of structural defects inside the granules also decreases, so the required efforts increase as the grinding process progresses:

- increasing the weight of elastic deformations of the material;
- the formation of secondary microcracks, which do not propagate, closing after the action of crushing efforts ceases;
- heating the shredded material;
- agglomeration of fine particles: this last phenomenon is harmful, because it consumes energy, having an effect opposite to breakage, reducing the specific surface of the product;
- sticking the fine material on the grinding organs, which dampens the shocks and reduces the grinding efforts;
- too advanced shredding of a part of the material.

The particles resulting from the crushing of the initial granules with different characteristics do not simultaneously reach sizes smaller than the prescribed

limit. The need to prolong the grinding operation until all the granules have the appropriate size also implies the appearance of fractions with too high fineness, especially in the case of high reduction ratios, such as those that are achieved in grinding processes, thus amplifying the effects of the phenomena listed above.

Given the technological importance of the grinding processes and the energy implications they bring, the present work sought to deepen the physics of these processes, namely: the determination of the energy consumption of the laboratory mill, the determination of the Blaine Specific Surface Area (SSA) and the variation between them.

### MATERIALS AND METHODS

To carry out the experiments, clinker material from a cement factory in Romania marked Clincher A was used. At the initial moment of the determinations, the sample was chemically characterized according to the requirements of SR EN 196–2:2013 – Test methods of cement. Part 2: For the chemical analysis of cement (Romanian Standard, 2013), the final clinker used to produce cement was type: CEM I 42.5 R, which is a Portland cement with high initial strength. The main constituents are Portland clinker (K) (95 %) and minor components (0–5%), (Holcim, 2021).

To carry out the experimental research, the CEPROCIM process was applied, which is based on the grinding of a batch of material in a laboratory mill with a rotating horizontal drum (Figure1) in two stages:

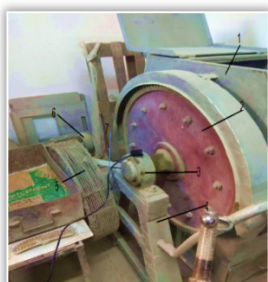
- the first stage with ball loading, (Figure 2);
- the second stage with a load of biconical bodies, (Figure 3).

The fineness of the material was periodically determined by the R009 residue and Blaine specific surface area (SSA). The first stage was considered completed when R009 is ~35% residue (R009 – residue on the 90 μm sieve). The energy consumption between the moments when the fineness of the material is determined was identified with the help of a wattmeter (the consumption was read directly from the meter). These consumptions were accumulated from the beginning of the determination and related to the mass of the batch (20 kg of clinker), calculating the specific energy consumption  $w_{li}$ , in the predetermined time unit of 10 minutes.

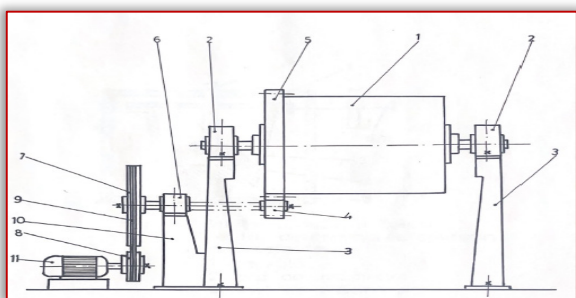
$$\text{Energy consumption} = \frac{\text{counter difference}}{\text{batch mass}} \cdot \frac{[\text{KWh}]}{[\text{kg}]} \quad (1)$$

The curves  $R009 = f(w_{li})$  and  $s = f(w_{li})$  were plotted. The grindability index is the specific energy consumption  $w_1$ , corresponding to a reference fineness, (Oprîș S., 1994). It can be evaluated by the specific Blaine surface and by sieving on a sieve of 009 mm (4900 mesh/cm<sup>2</sup> according to SR EN 196-6).

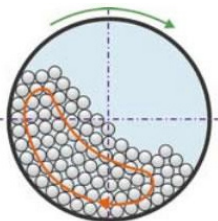
$$c_1 = \frac{w}{w_1} \quad (2)$$



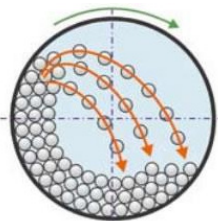
a)



b)



I.



II.

Figure 1 – Laboratory ball mill. a) principle diagram of the ball mill: 1 – mill body; 2 – mill bearings; 3 – mill supports; 4 – attack pinion; 5 – toothed crown; 6 – attack pinion bearing; 7, 8 – wheels for trapezoidal belts; 9 – trapezoidal belts; 10 – bearing support for the attack pinion; 11 – engine. b) operating regimes of ball mills, (Hanan Sankay Industrial Co., Ltd, 2022; Ene G. et al., 2005); I – cascade operation mode; II – cataract operation mode

The specific Blaine surface area was calculated according to relation (3) and is conventionally expressed in cm<sup>2</sup>/g, as:

$$S = \frac{K}{\rho} \cdot \frac{\sqrt{e^3}}{(1-e)} \cdot \frac{\sqrt{t}}{\sqrt{10 \cdot \eta}} \quad \frac{[\text{cm}^2]}{[\text{g}]} \quad (3)$$

where: K – device constant; e – porosity of the layer; t – measured time, in (s); ρ – cement density, in (g/cm<sup>3</sup>); η – air viscosity at the test temperature, in (Pa · s).

$$K = \frac{S_0 \rho_0 (1-e) \sqrt{10 \cdot \eta}}{\sqrt{e^3 \sqrt{t_0}}} \quad (4)$$

where: S<sub>0</sub> – the specific surface of the reference cement, (cm<sup>2</sup>/g); ρ<sub>0</sub> – volume mass of the reference cement, (g/cm<sup>3</sup>); t<sub>0</sub> – the average of three timed values of time, (s); η<sub>0</sub> – air viscosity corresponding to the average of three temperatures, in (Pa·s).

According to the CEPROCIM method, the load with grinding bodies, for the first experiment in the first phase of grinding (coarse) was according to the data presented in table 1:

Table 1. Load grinding bodies

Ø[mm] grinding balls	65–75	55–65	45–55	Total
G[kg] grinding balls	76,90	38,55	28,85	~144.3



Figure 2 – Grinding balls of different sizes

The final grinding (second phase – the fine one) was done with an equivalent load of bicones of ~144.3 kg. The bicones have the size of Ø 25 X 30 mm, in the laboratory ball mill. Grinding with bicones started in the ball mill, according to the CEPROCIM methodology, when the material residue on the 90 μm sieve (R90μm) reached around 30% (grinding balls were removed and bicones were inserted).



Figure 3 – Bicones

The same laboratory ball mill was used to simulate clinker grinding. Table 2 shows the properties of the materials used for the simulation and table 3 the parameters used for the simulation in the case of the previously mentioned ball mill. Clinker powder distribution, ball distribution, and wear were modeled using DEM. Dry grinding simulations were performed using a standard coefficient of restitution of 0.3 and a coefficient of friction of 0.75 (ball-ball and ball-material collisions), (Cleary, P.W., 2001). The charge consisted of powders and balls with a filling of 40% of the charge (by volume). The specific gravity of the support is equal to 2.7 kg/m<sup>3</sup>.

Table 2. Properties of materials used for simulation

Parameters	Value
Poisson ratio	0,3
Young modulus(N/m <sup>2</sup> )	1,8·10 <sup>11</sup>
Density (kg /m <sup>3</sup> )	7800

Table 3. Ball mill parameters used for simulation

Parameters	Value
Motor shaft power (kW)	0,37
Angular speed (rpm)	250
Effective disc diameter (mm)	140
Mill filling (%)	40
Mill speed (% critical speed)	10–100
Time step(s)	1,1·10 <sup>-4</sup>
Ball density (kg/m <sup>3</sup> )	7800
Ball size (mm)	60
Mill internal length (mm)	535
Internal diameter of the mill (mm)	540
Weight of grinding balls (kg)	144,3

## RESULTS

The stages of the experiment presented in this article, are:

- Clinker A (20kg) was sieved on the Ø =7 mm sieve, then the material remaining on the sieve was crushed in the jaw crusher Retsch BB100 to shred the clinker to pass it completely through the 7 mm sieve (Figure 4).



Figure 4 – Retsch BB 100 jaw crusher

- The content obtained was homogenized and subjected to sieving on particle size fractions (table 4), through a set of standardized sieves, according to SR EN 933-2 – 1998 (Romanian Standard, 1998), and later the particle size curve from Figure 5.

Table 4. The amount of material (pass percentage) rejected on the site of different sizes – clinker A

Sieve [mm]	Material remaining on the sieve [g], [%]		T [%]	R[%]
	p[g]	p[%]		
5	122,90	10,22	89,78	10,22
3	228,27	18,98	70,8	29,2
1	246,28	20,48	50,32	49,68
≤1	605,31	50,32	100	100
Total material	1202,76		–	

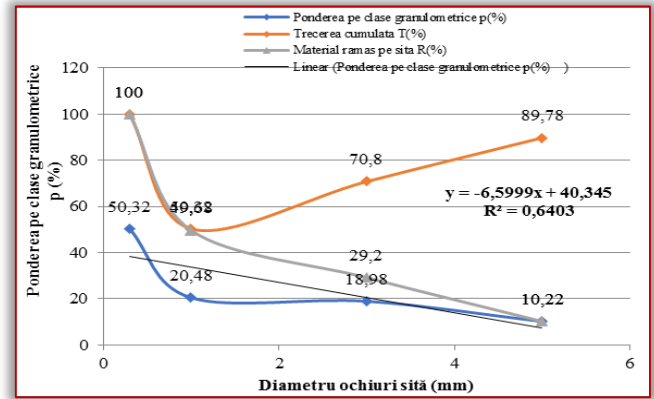


Figure 5 – Granulometric curve related to the amount of material–clinker A

## Experimental determinations regarding energy consumption when crushing clinker A

Clinker A (20 kg) was ground resulting in 10 samples (2 ball samples and 8 bicone samples). When the material residue on the 90 µm sieve (R<sub>90µm</sub>) reached around 30%, the grinding balls were removed and bicones were inserted. Thus, according to relation (1), the values presented in table 5 were obtained.

Table 5. Energy consumption related to grinding time – clinker A

No.crt.	Grinding time [min]	Counter display [kWh]	Counter difference [kWh] in time steps	Grinding bodies
0	0	7350421	0	Grinding balls
1	10	7350661	240	
2	20	7350882	221	
3	30	7351096	214	
4	40	7351314	218	
5	50	7351526	212	Bicones
6	60	7351746	220	
7	70	7351968	222	
8	80	7352196	228	
9	90	7352417	221	
10	100	7352642	225	

Table 6. Consumurile de energie raportat la timpul de măcinare – clincher A

No.crt.	Grinding time [min]	Resulting energy consumption [kWh/kg]	Cumulative energy consumption [kWh/kg]
1	10	10,7	10,7
2	20	10,9	21,6
3	30	10,6	32,2
4	40	11	43,2
5	50	11,1	54,3
6	60	11,4	65,7
7	70	11,05	76,75
8	80	11,25	88,00

After determining the energy consumption resulting from the grinding of clinker A, the variation of the specific crushing energy in the unit of time is shown in Figure 6.

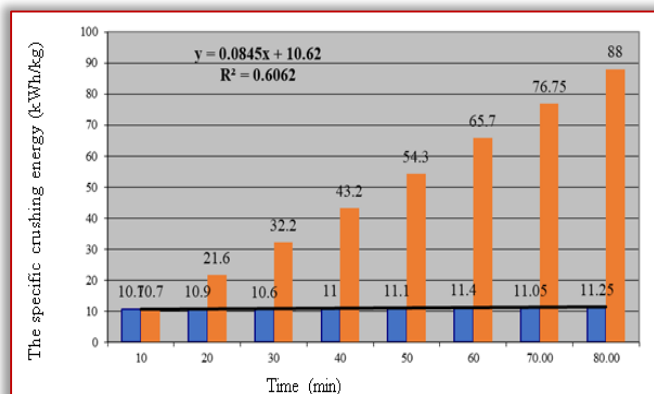


Figure 6 – Variation of specific clinker crushing energy A

**Experimental determinations regarding the specific surface area when grinding clinker**

To determine the Blaine Specific Surface Area (SSA) for different grinding times and different degrees of loading with balls and material, the calculation was made according to relation (3).

The equipment constant, K, was calculated according to relation (4), for a specific porosity value  $e = 0.50$ , and the test temperature  $t = 20 \pm 2^\circ\text{C}$ .

Thus, in table 7 the Blaine Specific Surfaces (SSA) resulting from the calculation were noted.

Table 7. SSA values and power consumption per unit of time

No.crt.	Grinding time [min]	Consumption meter indicator [kWh]	Grinding bodies	$R_{90\mu\text{m}}$ bile [%]	SSA bicones [ $\text{cm}^2/\text{g}$ ]
0	0	0	0	0	0
1	10	240	Grinding balls	51.68 %	–
2	20	221		33.6 %	–
3	30	214		–	2250
4	40	218	Bicones	–	2650
5	50	212		–	2830
6	60	220		–	3180
7	70	222		–	3520
8	80	228		–	3590
9	90	221		–	3700
10	100	225		–	3870

After determining the energy consumption when grinding type A clinker, the variation of the specific Blaine surface area (SSA) in the time unit was graphically represented (Figure 7).

A linear increasing variation of SSA with a slope of  $228.7 \text{ cm}^2/\text{g}/\text{min}$  is found.

**Determination of the grinding ability index which is represented by the specific energy consumption  $w_1$  corresponding to a reference fineness.**

Based on the results obtained and noted in table 8, the correlation coefficient diagram was drawn, figure 8, with the industrial mills ( $c_1$ ) in which the specific energy

consumption of the industrial mill was noted with  $w$ , in the assumption of action through the pinion–crown final group gear and speed reducer.

According to the value calculated by the cement factory  $W_{\text{consumption industrial mill}}$  is  $32.92 \text{ kWh}/\text{t}$ . This results in the following values for the correlation coefficient  $c_1$  (from formula 2) for the experimental determinations made

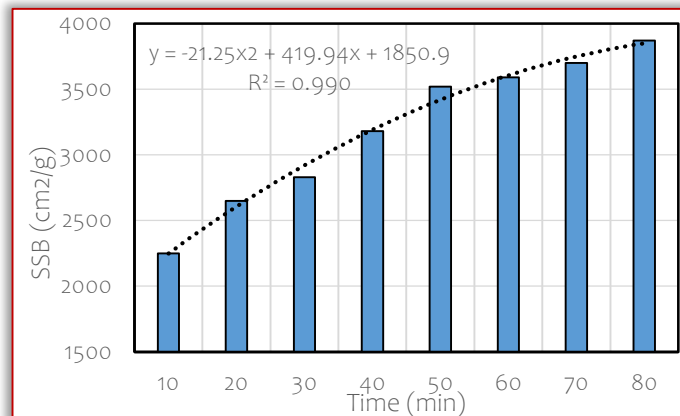


Figure 7 – Variation of blaine specific surface area when grinding clinker A with bicones mill

Table 8. Values of correlation coefficients  $c_1$  and energy consumption for clinker A

No.crt.	Grinding time [min]	Experimental result energy consumption [ $\text{kWh}/\text{t}$ ] clinker A	Correlation coefficient $c_1$ clinker A
1	10	10.7	3.08
2	20	10.9	3.02
3	30	10.6	3.11
4	40	11	2.99
5	50	11.1	2.97
6	60	11.4	2.89
7	70	11.05	2.98
8	80	11.25	2.93

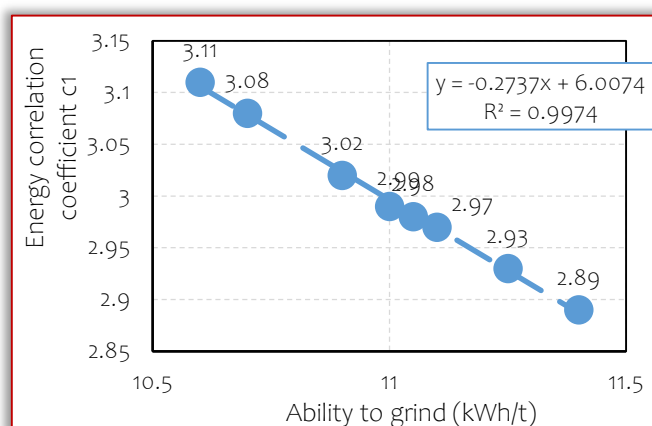


Figure 8 – Correlation of coefficient with industrial clinker mills A with grinding ability

Modeling assumptions are described starting from material identification (contact law), mill geometry and fill, and description of simulation and post–processing. During the simulation, all particles are considered and represented as spherical element. The stages of building a model are:

- cleaning the geometry (adding the components that will be simulated with their characteristics: balls, clinker), importing geometry;
- setting the dynamics of the model elements;
- setting the parameters of the model elements;
- setting the parameters of bulk materials.

Furthermore, the computer-aided design (CAD) geometry used for the DEM simulations is shown in Figure 9.

The geometry shows the characteristic regions of charge motion and the stochastic variability of the particle flow pattern. Thus, the particles are colored according to their speed. Figure 10 illustrates the different stages of particle breaking. The particle size distribution is mainly concentrated near the mill wall due to the high centrifugal accelerations caused by the drum motion.

With an increase in speed, the powders occupy almost the entire volume of the mill space. In addition, smaller particles, which receive a large amount of impact energy, travel in closed trajectories near the mill wall due to gravity.

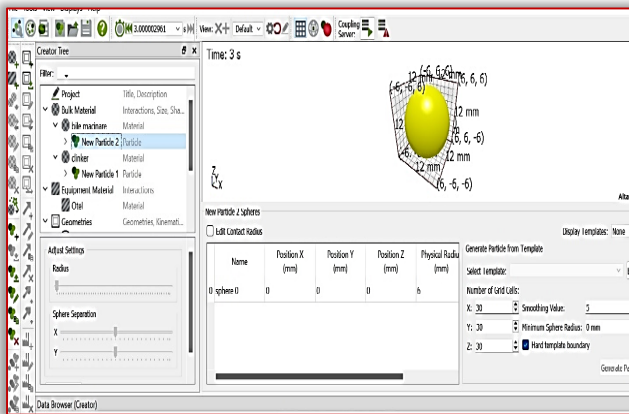


Figure 9 – Geometria de proiectare asistată de computer

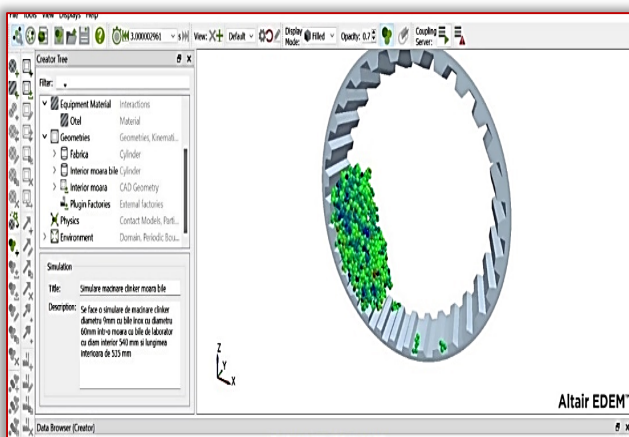


Figure 10 – Diferitele etape ale spargerii particulelor

Thus, the simulation results are consistent with those obtained by Hirosawa et. al. (2021). Furthermore, the velocity provides information about the charge movement. In the beginning (Figure 10), it seems that all the particles are uniformly distributed inside the load. As the mill speed increases (Figure 10), the particles

concentrate near the wall and are launched higher from the edge of the charge.

However, it means that the particles and balls are well mixed. Figure 11 shows particles moving at high speed, which produces high energy impacts during the grinding process. This can be explained by the fact that the flow of finer powder particles through the grinding media (mill walls-shields and balls). The number of collisions was also found to decrease with increasing energy per collision (Daraio, D., et al, 2020).

The variation of collision frequency with energy loss for different types of collisions (ball-particle-die, ball-ball, and ball-particle), collected from the DEM simulation, is shown in Figure 11. A reduction in the number of collisions and an increase in their magnitude can be observed.

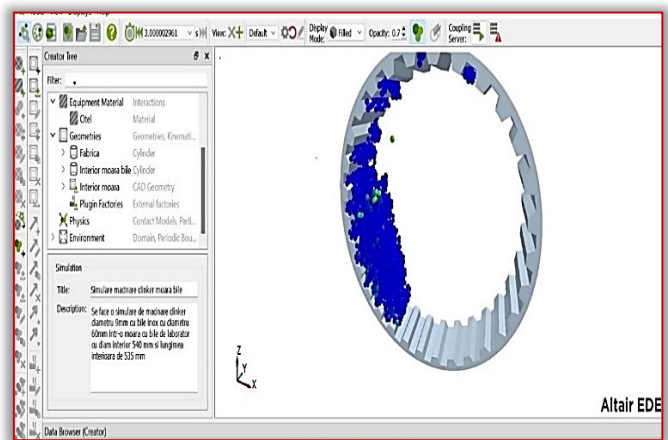


Figure 11 – Reducerea numărului de coliziuni

## CONCLUSIONS

After finishing the grinding, the clinker fell within the norms for the production of cement type CEM I 42.5 R. (having the Blaine specific surface around 3800 cm<sup>2</sup>/g), and the energy consumption is about 100 kWh/t.

The determination of the specific surface area (SSA) of the crushed material using the Blaine permeameter method is applicable for all cements defined in the EN 196-6: 2018 standard.

The simulation can be applied to calculate collision rates and impact energy spectra of industrial-scale ball mills and to understand particle behavior inside the mill

Raw material grinding plants in the cement industry are complex plants inside which, in addition to mechanical grinding processes, and thermo-technological processes through their drying take place. The major difficulty in the design, management, and optimization of the installation derives from the fact that in most cases the values of the input quantities and/or the environmental parameters register strong disturbances in a short time interval compared to the calculated values. For this reason, an analytical approach that covers all possible situations is not possible.

### Acknowledgement

This research was supported, among others, by Executive Unit for Financing Higher Education, Research, Development and Innovation, UEFSCDI, under the PNCDI III – Programme 2, sub-programme 2.1., as follows partially from: submission code PN-III-P2-2.1-PTE-2019-0446, funding contract no. 53PTE/23.09.2020, project title "Hydrophilic auto-chassis for high energy efficiency operation of interchangeable equipment intended for performing public utility work", acronym ASHEUP, research direction 3.Econano-technologies and advanced materials, subdomain Advanced materials and submission code PN-III-P2-2.1-PED-2019-4123, funding contract no. 380PED/23.10.2020, project title "Multifunctional hexa-rotors tricopter for precision farming", acronym 4.0-MHRT, project domain 1.Bioeconomics, subdomain 1.1.

### References

- [1] Cleary, P.W. (2001). Charge Behaviour and Power Consumption in Ball Mills: Sensitivity to Mill, Operating Conditions, Liner Geometry and Charge Composition. *International Journal of Mineral Processing*, Vol. 63, 79–114. [https://doi.org/10.1016/S0301-7516\(01\)00037-0](https://doi.org/10.1016/S0301-7516(01)00037-0)
- [2] Daraio, D., Villoria, J., Ingram, A., Alexiadis, A., Stitt, E.H., Munnoch, A.L. and Marigo, M. (2020). Using Discrete Element Method (DEM) Simulations to Reveal the Differences in the  $\gamma$ -Al<sub>2</sub>O<sub>3</sub> to  $\alpha$ -Al<sub>2</sub>O<sub>3</sub> Mechanically Induced Phase Transformation between a Planetary Ball Mill and an Attritor Mill. *Minerals Engineering*, 155, Article ID: 106374, <https://doi.org/10.1016/j.mineng.2020.106374>
- [3] Ene, G., Tomescu, Gh., Dobra, S. G. (2005). *Machines for shredding solid materials. Design guidelines*, Publisher: MatrixROM, ISBN: 973-685-868-5
- [4] Hiroswawa, F., Iwasaki, T. & Iwata, M. (2021). Particle Impact Energy Variation with the Size and Number of Particles in a Planetary Ball Mill. *MATEC Web of Conferences*, 333, 1–5. <https://doi.org/10.1051/mateconf/202133302016>
- [5] Opris, S. (1994). *Cement Industry Engineer's Handbook/ Manualul inginerului din industria cimentului*, Vol. I, Technical Publishing House, Cement National Institute CEPROCIM S.A./Institutul National de ciment CEPROCIM SA
- [6] \*\*\* Hanan Sankay Industrial Co.,Ltd (2022). <http://ro.sk-rockcrusher.com/grinding-mill/ball-mill.html>
- [7] \*\*\* Holcim, (2021). <https://www.holcim.ro/ro/produse-si-servicii/produse/ciment/cem-i-425-r>
- [8] \*\*\* Romanian Standard (1998). Tests to determine the geometric characteristics of the aggregates. Part 2: Particle size analysis – control sieve, nominal mesh sizes
- [9] \*\*\* Romanian Standard. (2013). Cement test methods. Part 2: Chemical analysis of cement (SR EN 196-2:2013). <https://magazin.asro.ro/ro/standard/111291>

**Note:** This paper was presented at ISB-INMA TEH' 2022 – International Symposium on Technologies and Technical Systems in Agriculture, Food Industry and Environment, organized by University "POLITEHNICA" of Bucuresti, Faculty of Biotechnical Systems Engineering, National Institute for Research-Development of Machines and Installations designed for Agriculture and Food Industry (INMA Bucuresti), National Research & Development Institute for Food Bioresources (IBA Bucuresti), University of Agronomic Sciences and Veterinary Medicine of Bucuresti (UASVMB), Research-Development Institute for Plant Protection – (ICDPP Bucuresti), Research and Development Institute for Processing and Marketing of the Horticultural Products (HORTING), Hydraulics and Pneumatics Research Institute (INOE 2000 IHP) and Romanian Agricultural Mechanical Engineers Society (SIMAR), in Bucuresti, ROMANIA, in 6–7 October, 2022.



**ISSN: 2067-3809**

copyright © University POLITEHNICA Timisoara,  
Faculty of Engineering Hunedoara,  
5, Revolutiei, 331128, Hunedoara, ROMANIA  
<http://acta.fih.upt.ro>